Parametric Tuning of Natural Frequencies of Tuning Fork Gyroscope

Rakesha Chandra Dash[1]([✉]) [iD], Rakesh Tirupathi[1], P. Krishna Menon[2],
and Ashok Kumar Pandey[1] [iD]

[1] Indian Institute of Technology Hyderabad,
Kandi, Sangareddy 502285, Telangana, India
[2] Research Centre Imarat, Hyderabad 500069, Telangana, India
{rakesh.chandradash,ashok}@mae.iith.ac.in

Abstract. The sequence of mode shapes play a vital role in designing a dual mass tuning fork gyroscope (TFG). To avoid loss of energy, a desired separation of frequencies between operating modes (out-of-phase drive and sense) and parasitic modes is required. Hence, regulation of mode shapes is an essential criterion in TFG design. In the present work, the influence of several crucial parameters such as coupling mechanisms and dimensions of folded beams on the in-plane frequencies are studied numerically by using finite element based COMSOL software.

Keywords: Tuning fork gyroscope · MEMS

1 Introduction

Microelectromechanical systems (MEMS) have been of significant interest for the design of inertial sensors because of their low cost, small size, and ruggedness and easy integration with the CMOS based signal conditioning readout interface [1–3]. MEMS inertial sensors like accelerometer and gyroscope find applications in consumer electronics, automobiles, defence, navigation, medical and other fields [4–7]. MEMS gyroscopes can be classified as tuning fork gyroscopes (TFG) [8–11], comb type [12,13], disk type [14,15], and wine glass type gyroscopes [16]. Applications like inertial navigation systems for ships, aircraft, submarines, and other spacecraft require very high sensitivity and resolution [17–19]. However, the resolution of inertial MEMS devices is mainly limited by Brownian noise in micromechanical structures and interface electronics circuit noise [20–22]. Low mechanical sensitivity of MEMS devices may cause the electronics noise to dominate and limit the resolution [23]. This challenge can be addressed by exploiting different techniques like mechanical amplification using

compliant mechanisms, geometric anti-spring design, mechanical coupling, and mode-localized [26] designs toward the sensitivity improvement of MEMS gyroscope. However, while using any of these techniques, frequencies of gyroscopes also get affected. The variation of frequencies due to coupling mechanisms and their dimensions, we take tuning fork gyroscope (TFG) from [24] for further analysis.

The TFG is mainly categorized as single mass gyroscope, dual-mass gyroscope and quad mass gyroscope. Single mass gyroscope consists of an overlap between drive and sense vibrations, which requires a complex interface to distinguish the required Coriolis force. In the case of a quad mass gyroscope, the mismatch between the four masses and stiffness introduces unwanted errors to the measurement. In the case of a dual-mass gyroscope, the two proof masses vibrate either in-phase or out-of-phase to capture the Coriolis force. Among these two approaches, out-of-phase oscillations (operating modes) eliminate the common vibrations.

Therefore, it is a necessary criterion to design dual-mass TFG such that the out-of-phase drive and sense modes are away from other modes to reduce interference. The present study utilizes various important parameters to regulate the in-plane mode shapes to get the desired output.

2   Dual Mass Tuning Fork Gyroscope

Dual mass tuning fork gyroscopes consist of two masses oscillating in out-of-phase mode. The basic design of the gyroscope is shown in the Fig. 1. The performance of the TFG can be changed based on the coupling mechanisms that will be described in further sections. In this section, various critical design parameters and their effects on modulating natural frequencies are studied. The fundamental frequencies and mode shapes are found out by using finite element based COMSOL software.

Table 1. Element convergence study for TFG with spring type coupling

| Element numbers	1,013,967	541,457	395,478	305,898	240,391
Element size (Lowest, highest)	(1,30)	(3,50)	(10,50)	(15,70)	(20,90)
1st mode (Hz)	8960	8963	8986	8997	9011
2nd mode (Hz)	9401	9406	9428	9440	9452
3rd mode (Hz)	10,587	10,591	10,612	10,624	10,637
4th mode (Hz)	14,001	14,020	14,038	14,058	14,067

2.1   Dual Mass TFG with Spring Coupling

The design of TFG with spring coupling is shown in Fig. 1. A convergence study based on the natural frequencies is first done to decide the minimum element

size without compromising the accuracy of the solution. COMSOL software is used for this purpose and results are shown for different element sizes in Table 1. An element size of (1,30) is selected for the further modal analysis in Fig. 2. The Y-axis and X - axis are taken as drive and sense directions, respectively. In the first mode, an in-phase motion of the mass is observed in the sense direction. An out-of-phase motion in the sense direction is seen in the second mode. The third mode consists of an out-of-phase drive motion and the fourth mode is in-phase drive motion.
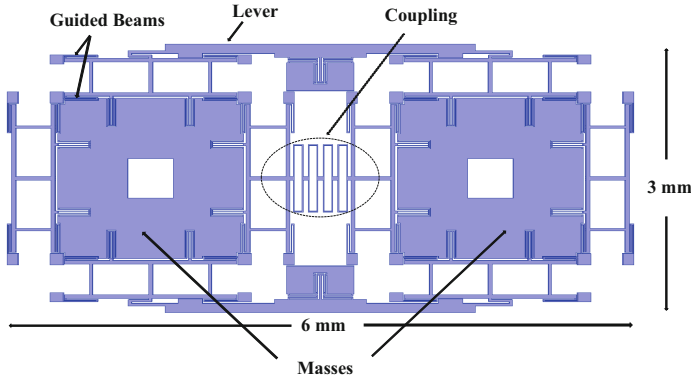
(a)
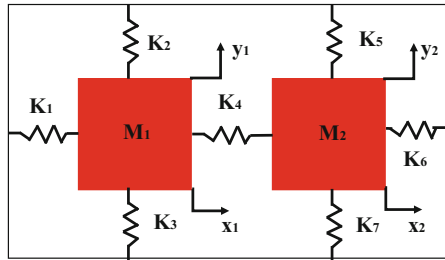
(b)

Fig. 1. (a) Dual mass TFG with spring coupling and (b) its lumped mass model

A free body diagram of the whole structure is drawn in Fig. 1b to derive the analytical expressions. Each mass possesses of 2 degree of freedom (dof) and, hence, the system will have 4 dofs. Therefore, there will be four governing differential equations given in Eqs. 1–4. The force F_1, F_2, F_3, F_4 are applied forces for each degree of freedoms. The stiffness K_1, K_2, K_3, K_4, K_5, , K_6 and K_7 are found analytically. There are three type of spring used in this gyroscope shown in Fig. 3. The stiffness of the guided beam is given by $K_G = 12EI_1/L_1^3$, where EI is Flexural rigidity of the beam. For the shorter beam like one shown with the length L_2 in Fig. 3b, the stiffness is obtained from $K_B = 3EI_1/L_1^3$.
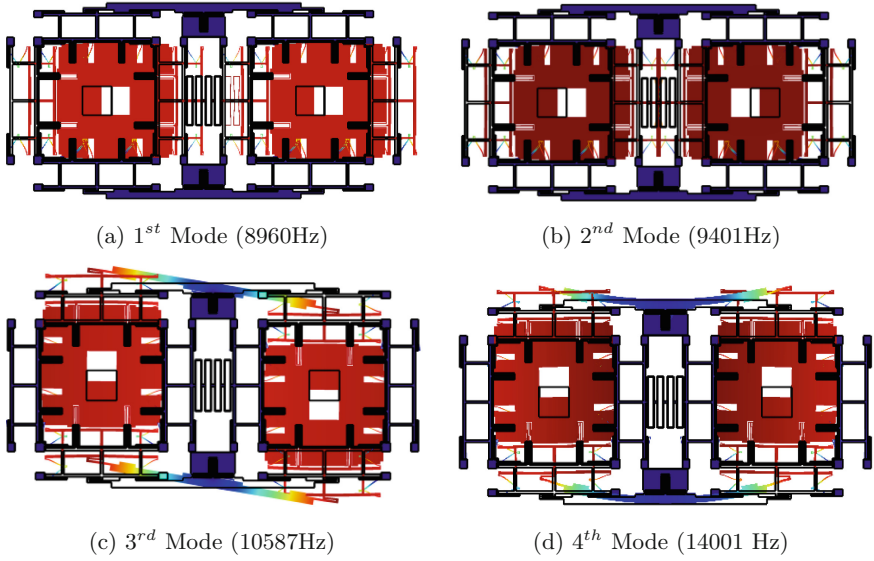
(a) 1st Mode (8960Hz)

(b) 2nd Mode (9401Hz)

(c) 3rd Mode (10587Hz)

(d) 4th Mode (14001 Hz)

Fig. 2. Mode shapes of TFG with spring coupling

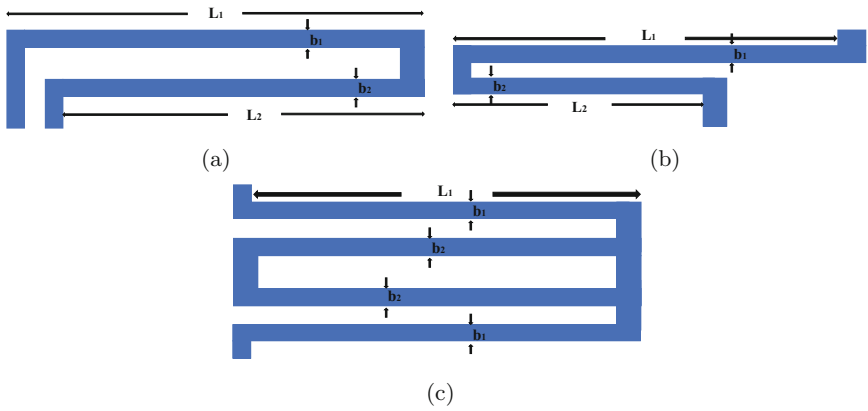(a)   (b)

(c)

Fig. 3. Various type of springs used in TFG

After the calculation of the beam stiffness, series and parallel combinations are used to find the total stiffness of Fig. 3a–c structures.

$$M_1\ddot{x}_1 + K_1 x_1 + K_4(x_2 - x_1) = F_1, \tag{1}$$

$$M_2\ddot{x}_2 + K_6 x_2 + K_4(x_1 - x_2) = F_2, \tag{2}$$

$$M_1\ddot{y}_1 + (K_2 + K_3)y_1 = F_3, \tag{3}$$

$$M_2\ddot{y}_2 + (K_5 + K_7)y_2 = F_4. \tag{4}$$

The above equations are solved for eigen values and the natural frequencies are compared with COMSOL solutions in Table 2. The difference between the analytical and COMSOL is due to the consideration of simplified model and guided beam assumptions in the stiffness calculation. It is vital to regulate these mode shapes according to our need. Various regulating parameters and their effects on the sense and drive modes are described. Regulating in-phase sense mode needs a different approach so it will be described at the last.

Table 2. Comparison of natural frequencies from analytical model and COMSOL

Analytical (Hz)	COMSOL (Hz)
9275.6	
	8960
9681.1	
	9401
10,062	10,587
10,126	14,001

(a) Modulating Out-of-Phase Sense Mode The dimensions of coupling spring play a significant role in deciding the 2nd mode frequency. The length of spring effects the 2nd mode drastically and can be seen from Fig. 4a. The increase in coupling spring length reduces the stiffness in out-of-phase sense mode, thus, it reduces the corresponding frequency, while, the other modes are unaffected.
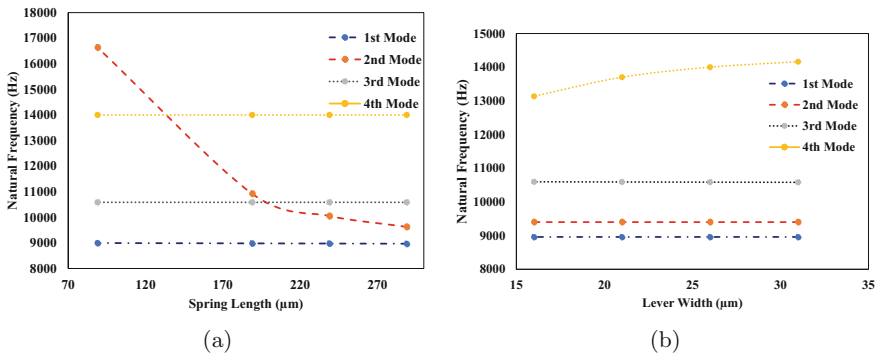

(a)   (b)

Fig. 4. Variation of natural frequencies for dual mass TFG with spring coupling with (a) change in length of spring (a) change in width of lever

(b) Modulating Out-of-Phase Drive Mode The out-of-phase drive mode can be regulated by changing dimensions of the folded beams in drive direction or

by changing various coupling mechanisms. The other coupling mechanisms used in our study are shown in Fig. 5. It can be observed by comparing the mode shapes in Figs. 1, 6, and 7 that out-of-phase drive mode has shifted its position from 2nd mode to 3rd mode for elliptical and diamond coupling, respectively. Thus, coupling mechanisms can influence out-of-phase drive mode and out-of-phase sense mode drastically.
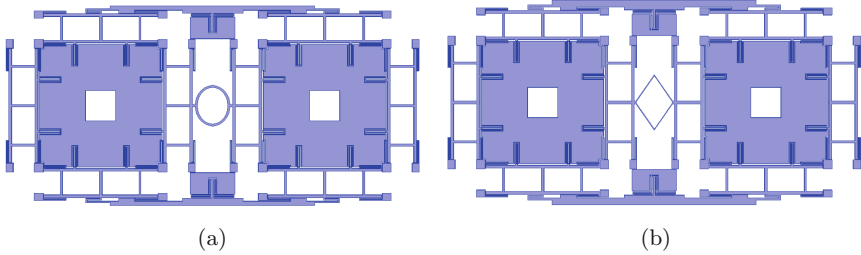

(a)   (b)

Fig. 5. Dual mass TFG with (a) elliptical coupling (a) diamond coupling

(a) 1st Mode (8969 Hz)   (b) 2nd Mode (9015 Hz)

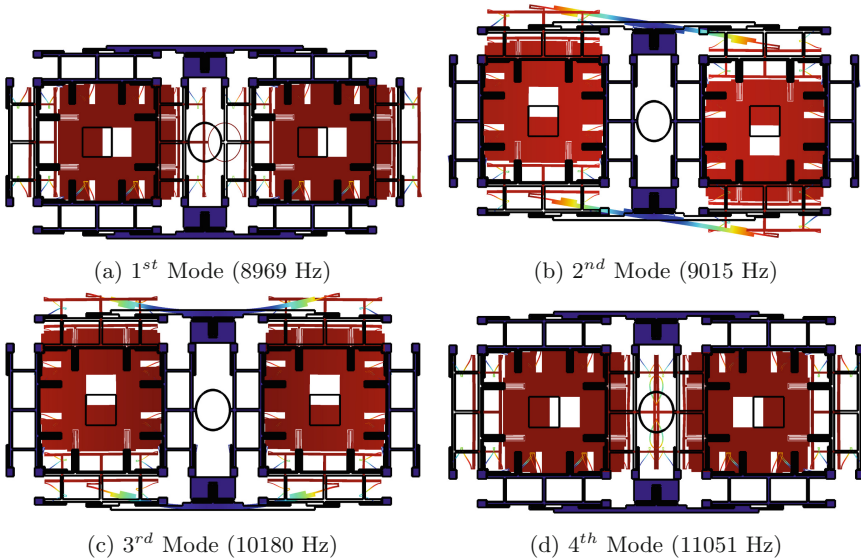(c) 3rd Mode (10180 Hz)   (d) 4th Mode (11051 Hz)

Fig. 6. Modeshapes of TFG with elliptical coupling

(c) Modulating In-Phase Drive Mode The dimensions of lever can be changed to regulate the in-phase drive mode in TFG as shown in Fig. 4b. It can be seen that with increase in the width of the lever, the stiffness of in-phase drive mode increases, and, hence the natural frequency also increases.
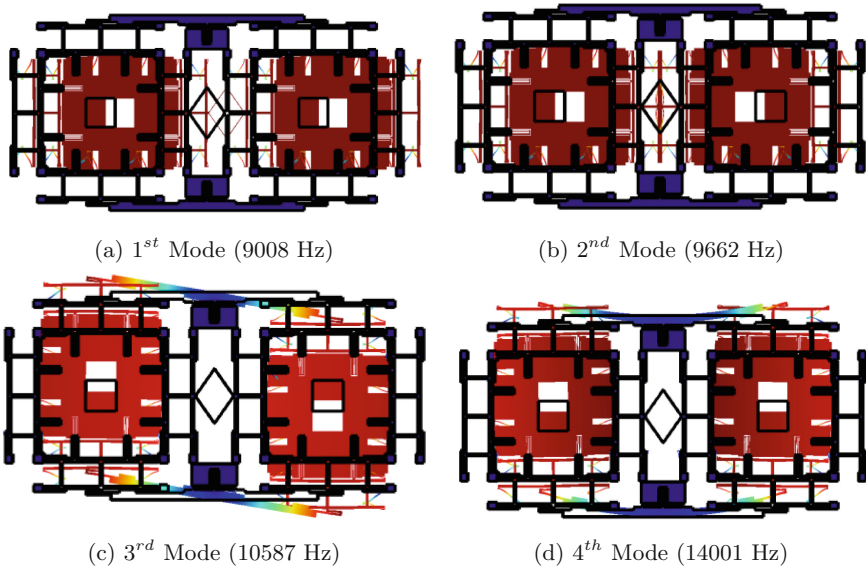
(a) 1st Mode (9008 Hz)

(b) 2nd Mode (9662 Hz)

(c) 3rd Mode (10587 Hz)

(d) 4th Mode (14001 Hz)

Fig. 7. Mode shapes of TFG with diamond coupling

(d) Modulating In-Phase Sense Mode It can be seen form above analysis
that in-phase sense mode remains the same irrespective of change in parameters.
Therefore, a special folded beam [25] is used as shown in Fig. 8. These beams will
only affect the in-phase sense mode during the motion. There is very small effect
on the frequency of out-of-phase sense mode. Consequently, it can be seen from
the Fig. 9 that the frequency of first mode is increased 21,168 Hz from 9008 Hz
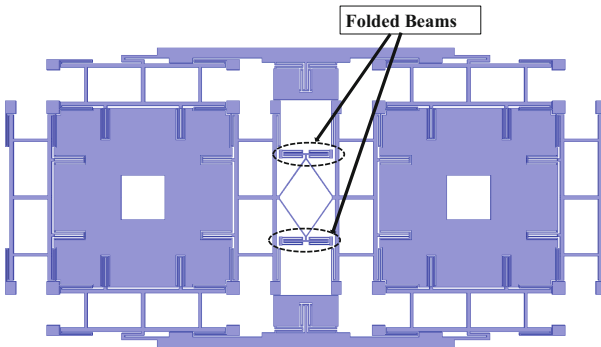(see Fig. 7).

Folded Beams

Fig. 8. Attachment of additional folded beam to regulate in-phase sense mode

(a) 1st Mode (10588 Hz)

(b) 2nd Mode (10689 Hz)

(c) 3rd Mode (14001 Hz)
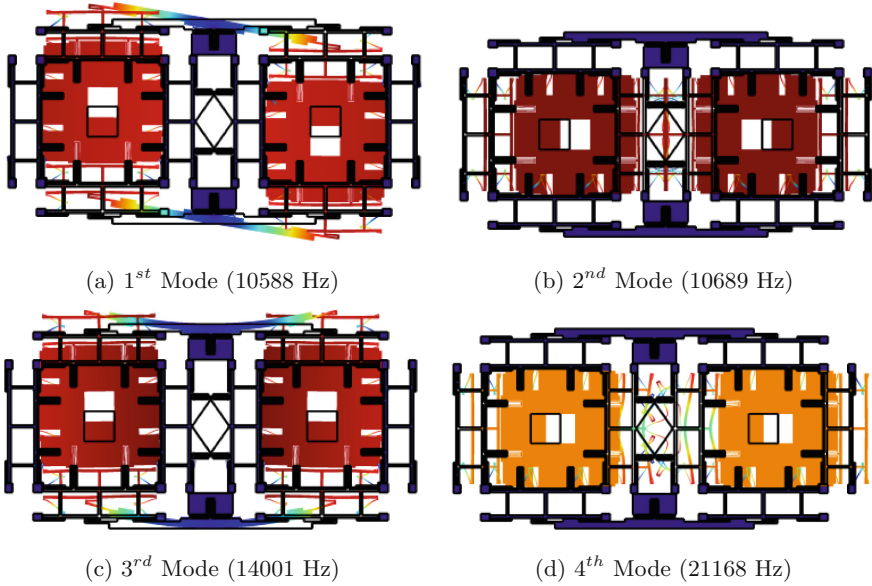
(d) 4th Mode (21168 Hz)

Fig. 9. Mode shapes of TFG with diamond coupling with folded beam attachments

3   Conclusions

In this study, the modal analysis of dual mass TFG is done by the help of COMSOL software and validated by using analytical modeling. The effects of various coupling mechanisms and folded beams dimensions on mode shapes are explored. The main aim is to regulate the mode shapes of the TFG. It is found that in-phase drive, out-of-phase drive and out-of-phase sense mode shapes can easily be interchanged by changing the coupling mechanisms and dimensions of the guided beams. The modulation of the in-phase sense mode shape require special guided beam arrangements near the coupling mechanism. These mechanisms only effects the in-phase sense mode.

References

1. Yazdi, N., Ayazi, F., Najafi, K.: Micromachined inertial sensors. Proc. IEEE **86**(8), 1640–1659 (1998)
2. Xia, D., Yu, C., Sensors, L.K.: undefined,: the development of micromachined gyroscope structure and circuitry technology. Mdpi. Com. **14**, 1394–1473 (2014)
3. Söderkvist, J.: Micromachined gyroscopes. Sens. Actuators A Phys. **43**, 65–71 (1994)

4. Passaro, V.M.N., Cuccovillo, A., Vaiani, L., De Carlo, M., Campanella, C.E.: Gyroscope technology and applications: a review in the industrial perspective. Sensors **17**, 2284 (2017)
5. Ma, W., Lin, Y., Liu, S., Zheng, X., Jin, Z.: A novel oscillation control for MEMS vibratory gyroscopes using a modified electromechanical amplitude modulation technique. J. Micromech. Microeng. Iopscience. Iop. Org. 27(2) (2016)
6. Pang, G., Liu, H.: Evaluation of a low-cost MEMS accelerometer for distance measurement. J. Intell. Robot. Syst. Theory Appl. **30**, 249–265 (2001)
7. Wu, J., Zhou, Z., Fourati, H., Cheng, Y.: A super fast attitude determination algorithm for consumer-level accelerometer and magnetometer. IEEE Trans. Consum. Electron. **64**(3), 375–381 (2018)
8. Nguyen, M.N., Ha, N.S., Nguyen, L.Q., Chu, H.M., Vu, H.N.: Z-axis micromachined tuning fork gyroscope with low air damping. Micromachines **8**, 42 (2017)
9. Yang, C., Li, H.: Digital control system for the MEMS tuning fork gyroscope based on synchronous integral demodulator. IEEE Sens. J. **15**(10), 5755–5764 (2015)
10. Guan, Y., Gao, S., Liu, H., Jin, L., Niu, S.: Design and vibration sensitivity analysis of a MEMS tuning fork gyroscope with an anchored diamond coupling mechanism. Sensors **16**, 468 (2016)
11. Prikhodko, I., Zotov, S., Trusov, A., Shkel, A.M.: Foucault pendulum on a chip: rate integrating silicon MEMS gyroscope. Elsevier. **177**(2012), 67–78 (2012)
12. Tatar, E., Mukherjee, T., Fedder, G.K.: Stress effects and compensation of bias drift in a MEMS vibratory-rate gyroscope. J. Microelectromech. Syst. 26(3), 569–579
13. Park, B., Han, K., Lee, S., Yu, M.-J.: Analysis of compensation for a g-sensitivity scale-factor error for a MEMS vibratory gyroscope. Iopscience. Iop. Org **25**(11), 115006 (2015)
14. Sonmezoglu, S., Alper, S., Akin, T.: An automatically mode-matched MEMS gyroscope with wide and tunable bandwidth. Ieeexplore. Ieee, Org (2014)
15. Zhou, X., Xiao, D., Wu, X., Wu, Y., Hou, Z., He, K., Li, Q.: Stiffness-mass decoupled silicon disk resonator for high resolution gyroscopic application with long decay time constant (8.695 s). Appl. Phys. Lett. 109 (2016)
16. Guan, Y., Gao, S., Jin, L., Cao, L.: Design and vibration sensitivity of a MEMS tuning fork gyroscope with anchored coupling mechanism. Microsyst. Technol. 22, 247–254
17. Nusbaum, U., Rusnak, I., Klein, I.: Angular accelerometer-based inertial navigation system. Navigation. **66**, 681–693 (2019)
18. He, Q., Zeng, C., He, X., Xu, X., Lin, Z.: Measurement, undefined 2018, Calibrating accelerometers for space-stable inertial navigation systems at system level. Elsevier
19. El-Sheimy, N., Youssef, A.: Inertial sensors technologies for navigation applications: state of the art and future trends. Satell. Navig. 1 (2020)
20. Petritoli, E., Leccese, F., Leccese, M.: Inertial navigation systems for UAV: Uncertainty and error measurements. Ieeexplore. IEEE, Org (2019)
21. Handtmann, M., Aigner, R., Meckes, A., Wachutka, G.K.M.: Sensitivity enhancement of MEMS inertial sensors using negative springs and active control. Sens. Actuators A Phys. **97–98**, 153–160 (2002)
22. Masu, K., Machida, K., Yamane, D., Ito, H., Ishihara, N., Chang, T.-F.M., Sone, M., Shigeyama, R., Ogata, T., Miyake, Y.: (Invited) CMOS-MEMS based microgravity sensor and its application. ECS Trans. **97**, 91–108 (2020)
23. Gabrielson, T.G.: Mechanical-thermal noise in micromachined acoustic and vibration sensors. Ieeexplore. IEEE Trans. Electronic, Dev (1993)

24. Cao, L., Li, J., Liu, X., Sun, F.Y.: Research on an anchor point lever beam coupling type tuning fork micro-gyroscope. Int. J. Precis. Eng. Manuf. **21**, 1099–1111 (2020)
25. Li, Z., Gao, S., Jin, L., Liu, H., Guan, Y., Peng, S.: Design and mechanical sensitivity analysis of a MEMS tuning fork gyroscope with an anchored leverage mechanism. Sensors (Basel). **19**(16), 3455 (2019)
26. Bukhari, S.A.R., Saleem, M.M., Hamza, A., Bazaz, S.A.: A novel design of high resolution MEMS gyroscope using mode-localization in weakly coupled resonators. IEEE Access **9**, 157597–157608 (2021)